

On the “Forbidden” Ferroelastic Domain Structure in $Rb_{2x}Tl_{2(1-x)}Cd_2(SO_4)_3$ Crystals ($x=0.1, 0.2$ and 0.3). Optical Microscopic Observations

A. Say, Yu. Vasylykiv, I. Girnyk and R. Vlokh

Institute of Physical Optics, 23 Dragomanov St., 79005 Lviv, Ukraine,
e-mail: vlokh@ifp.lviv.ua

Received:14.06.2006

Abstract

Ferroelastic (FE) domain structure and movement of phase boundaries have been studied in the course of phase transitions in $Rb_{2x}Tl_{2(1-x)}Cd_2(SO_4)_3$ crystals. The reasons for the appearance of so-called “forbidden” domain structure in FE langbeinites have been found. We have shown that two types of conjugated domain walls can appear. In some cases, the phase boundaries could play a part of domain walls.

Key words: ferroelastics, domain structure, “forbidden” walls, langbeinite crystals

PACS: 77.80.Dj , 78.20.Fm

Introduction

$Rb_2Cd_2(SO_4)_3$ and $Tl_2Cd_2(SO_4)_3$ crystals (abbreviated respectively as RCS and TCS further on) belong to a family of langbeinite mineral with the general formula $M_2^+M_2^{++}(SO_4)_3$, where M_2^+ and M_2^{++} are monovalent and bivalent metal ions, respectively [1–3]. These crystals undergo a common sequence of phase transitions (PTs), namely the PTs with the change of point symmetry $23F2F1F222$ (the change of the

space groups being $P2_13F \leftrightarrow P2_1F \leftrightarrow P1F \leftrightarrow P2_12_12_1$) [4,5]. The PT into orthorhombic phase is purely ferroelastic (FE), while the transformations into monoclinic and triclinic phases are ferroelectric-FE. In our recent papers [6,7] we have reported the x,T -phase diagram obtained for the mixed $Rb_{2x}Tl_{2(1-x)}Cd_2(SO_4)_3$ (or RTCS) crystals. It has been found that all the mixed crystals have the same sequence of PTs. The temperatures of the corresponding PTs are collected in Table 1.

One of interesting peculiarities of the PTs in langbeinite crystals is that the domain

Table 1. PT temperatures for RTCS crystals [6].

x	T_{c1} , K ($P2_13 \leftrightarrow P2_1$)	T_{c2} , K ($P2_1 \leftrightarrow P1$)	T_{c3} , K ($P1 \leftrightarrow P2_12_12_1$)
0.1	128	124	101
0.2	127	113	98
0.3	133	119	102
0.4	126	112	97
0.5	125	115	95
0.6	~117	92	80
0.7	~124	106	97
0.8	~97	92	87

structure, which appears at the PT into FE phase with the point symmetry 222 , is completely forbidden by mechanical compatibility conditions [8]. Nevertheless, we have detected the appearance of domain structure at the direct PT into FE phase $23F222$ in each of the row of mixed $K_2\text{Cd}_{2x}\text{Mn}_{2(1-x)}(\text{SO}_4)_3$ crystals, including pure $K_2\text{Cd}_2(\text{SO}_4)_3$ and $K_2\text{Mn}_2(\text{SO}_4)_3$ [9–15]. It has been found that the FE domains are separated by thick domain walls that manifest the properties of cubic paraelastic phase and have the orientation $\{110\}$ (see, e.g., [13]). The observed phenomena have been explained as a result of remaining twin walls that exist in the cubic phase with the symmetry 23 between enantiomorphous states appearing due to hypothetical PT with the symmetry change $\bar{4}3mF23$ [13]. The latter conclusion has been proven by experimental observations of optical activity variation within samples in the cubic phase 23 [11]. We have also observed the so-called conjugated domain walls, which should assemble orthogonal pair of walls with the $\{110\}$ walls. However, these walls are inclined with respect to those with the orientation $\{110\}$ by a rather large angle ($>10^\circ$). For example, this angle achieves 19° in case of $K_2\text{Mn}_2(\text{SO}_4)_3$ crystals [9]. Notice that such a large deviation from mutually orthogonal positions of the conjugated domain walls cannot be explained as a manifestation of spontaneous distortion, since the latter does not normally exceed tenth of degree (see [16]). It is necessary to recall that, in case of the domain walls observed in $K_2\text{Cd}_{2x}\text{Mn}_{2(1-x)}(\text{SO}_4)_3$ crystals, the domains on both sides of the domain wall are in contact with the cubic paraelastic phase. Therefore, this domain wall can be also considered as a phase boundary. In some cases we have observed transformations of the phase boundaries moving from the two opposite sides of samples to the domain walls, when the phase transformation is completed

[10]. Nonetheless, there still remains a number of unresolved problems:

1. Can the inclined walls be considered as conjugated walls and what is a nature of the observed non-orthogonality of these “conjugated” walls? Could these inclined domain walls be also considered as remaining twin walls?

2. Which is behaviour of the “forbidden” domain walls in the case of indirect PT into the phase 222 ? In particular, would the region of paraelectric-paraelastic phase play also a part of domain walls?

In the present paper we solve these problems on the basis of studies for the FE PT in RTCS crystals.

Experimental results

The domain structure was observed using polarization Karl-Zeiss microscope supplied with a cooling cell. The temperature was controlled by thermocouple and changed with the rate of 1 K/min .

For the case of cooling run and the crystals with $x = 0.1, 0.2$ and 0.3 compositions, we have observed a movement of phase boundary between the cubic and monoclinic phases and the triclinic and orthorhombic phases. The PT between the monoclinic and triclinic phases is accompanied only by a slight reconstruction of domain structure, without well-defined orientation of the phase front. The typical domain structure of the triclinic phase is shown in Fig. 1a.

The process of FE phase transformation in the mixed RTCS crystals with $x = 0.3$ is shown in Fig. 1 and 2. It has been found that the FE phase always appears as a single-domain state in the samples with $x = 0.1, 0.2$ and 0.3 (see Fig. 1b, Fig. 3c, d and Fig. 4). The pure $\text{Ti}_2\text{Cd}_2(\text{SO}_4)_3$ crystals and the mixed $\text{K}_{1.6}\text{Mn}_{0.4}\text{Cd}_2(\text{SO}_4)_3$ crystals, where the FE domain walls occurring below the FE PT have

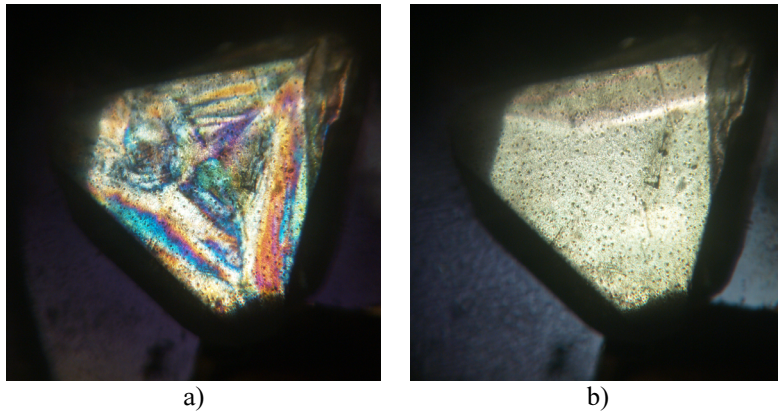


Fig. 1. Domain structure for RTCS crystals ($x = 0.3$) of $\langle 111 \rangle$ orientation: (a) multidomain state in the triclinic phase $P1$ ($T \approx 110K$) and (b) single-domain state in the FE phase $P2,2,2,1$ ($T \approx 90K$).

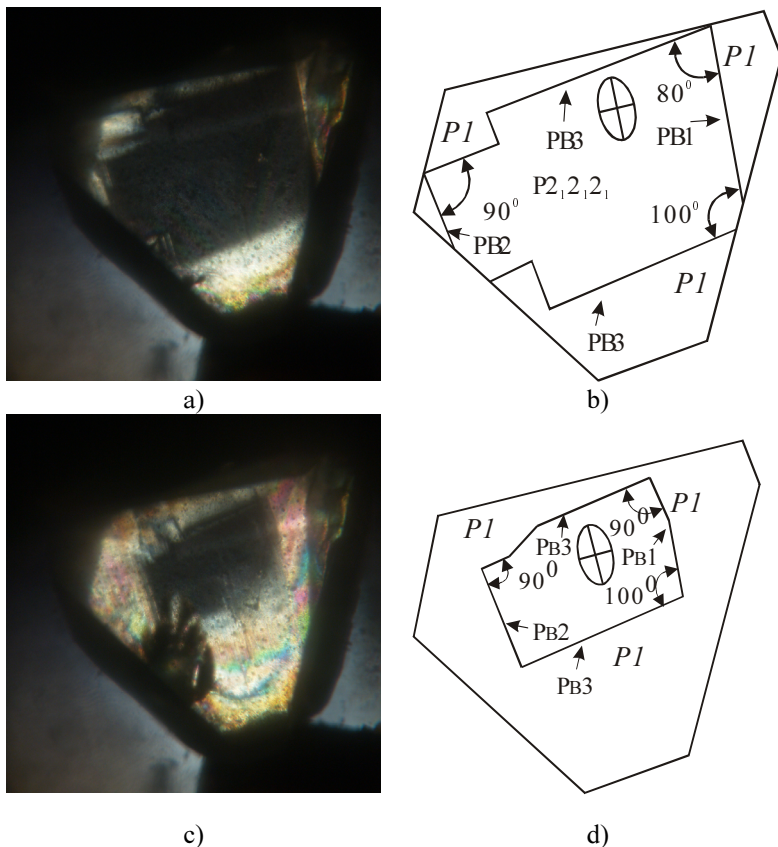


Fig. 2. Phase boundaries at the FE PT ($T_{c3} \approx 102K$) in RTCS crystals ($x = 0.3$) of $\langle 111 \rangle$ orientation: (b) and (d) represent schematically microphotographs (a) and (c), respectively. The region of FE phase is in the 'extinction' position between crossed polarizers and (a), (b) and (c), (d) correspond to sequential heating runs.

exactly the orientation $\{110\}$ [11,17], are the only exceptions. Such the behaviour is explained by exact elastic compatibility and a unique lattice parameter change taking place in the FE phase of $K_{1.6}Mn_{0.4}Cd_2(SO_4)_3$ and, probably, $Tl_2Cd_2(SO_4)_3$ (two of the diagonal components of spontaneous deformation tensor have the same magnitude and the opposite signs, while the third component is equal to zero). Notice that in $Tl_2Cd_2(SO_4)_3$ crystals [17] we have not actually observed the appearance of mechanical stresses between the domains and the appearance of the cubic phase as domain walls.

The process of disappearing of the FE phase in the heating regime is presented in Fig. 2. Three clear phase boundaries are visible in Fig. 2a, which move from different sides of the sample. The phase boundary PB1 is oriented parallel to the principal axis of optical indicatrix and so to the plane (110). The phase boundaries PB2 and PB3 are mutually orthogonal, though inclined with respect to the (110) plane by the angles of $\sim 10^\circ$ and $\sim 100^\circ$, respectively. The phase boundaries PB2 and PB3 can be therefore considered as the conjugated orthogonal boundaries. We have not observed a boundary

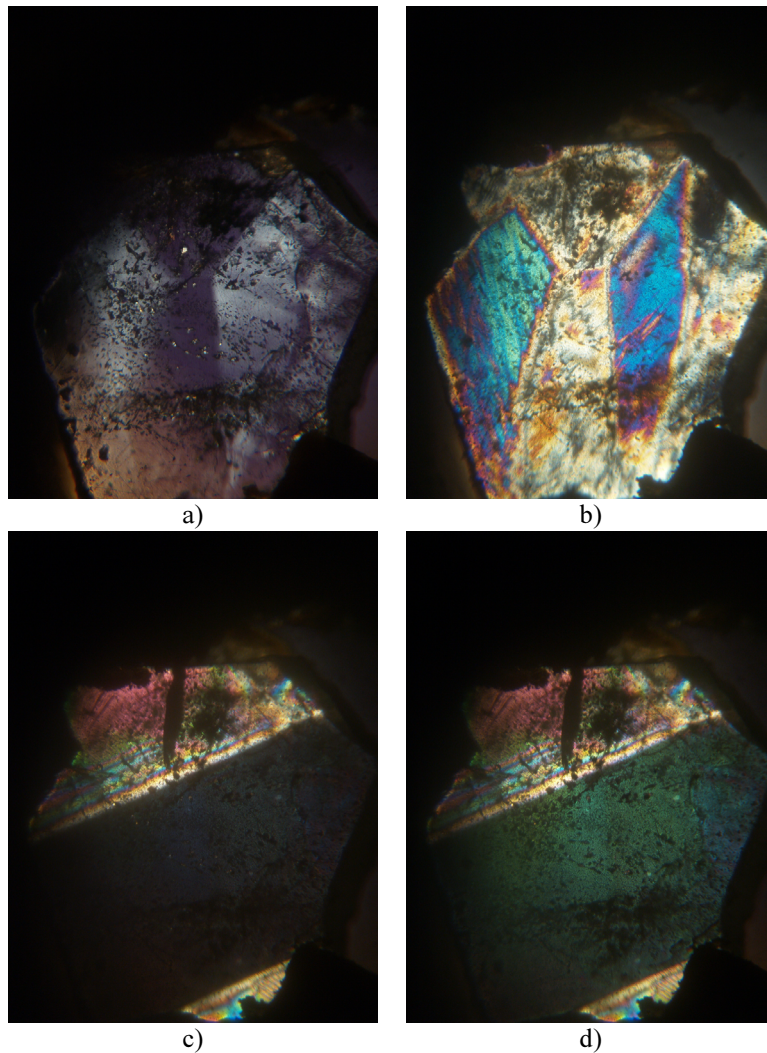


Fig. 3. Residual twins in the phase $P2_13$ at room temperature (a), domain structure in the triclinic $P1$ phase at $T \approx 107\text{K}$ (b), and the phase boundary between the triclinic and orthorhombic FE phase at $T_{c3} = 98\text{K}$ (c, d) in the RTCS crystals ($x = 0.2$) of $\langle 111 \rangle$ orientation. In figures (c) and (d) regions of the FE phase and the triclinic phase, respectively, are in the ‘extinction’ position. Figure (e) represents a schematic view of Fig. 3c.

orthogonal to PB1, but there are no limitations on its appearance. Moreover, the PB1 boundary is parallel to the domain walls observed in the other FE langbeinites. The inclined boundaries (the boundaries with similar inclinations to the (110) plane) have also been observed in langbeinites as the domain walls. The phase boundaries slightly change their orientation with further heating (see Fig. 2c and 2d). The cracks appear near the phase boundaries, thus justifying stresses in the vicinity of the boundaries. On the other hand, we have observed the appearance of conjugated boundary orthogonal to the PB1. It follows from the results of our observations that the phase boundaries can possess the two equilibrium positions: the pairs of conjugated boundaries, one of which is exactly parallel to (110) plane, and the pair of conjugated

boundaries, one of which is inclined with respect to (110) plane by $\sim 10^\circ$. The mechanical stresses and the appropriate cracks can slightly change the orientation of the phase boundaries ($\sim 6^\circ$).

For the cubic phase of RTCS crystals with $x = 0.2$, we have observed a residual twinning at the room temperature (Fig. 3a). Similarly to the PT occurring in crystals with the $x = 0.3$ composition, the PT into the monoclinic phase taking place in crystals with $x = 0.2$ is accompanied by a phase boundary movement, while the PT to the triclinic phase manifests itself only in the domain structure changes. It is interesting that the orientation and location of the remaining twin walls at the room temperature coincide with those of the domain walls of triclinic domain structure (Fig. 3b). In

the course of PT into the FE phase, we have observed a movement of the phase boundary, which is inclined with respect to the sample surface. This inclination is indicated by the interference fringes observed in the vicinity of the phase boundary (see Fig. 3c and 3d). The angle between the trace of the phase boundary on (111) plane and the principal axis of optical indicatrix in the FE phase is equal to 30° . Then the phase boundary is parallel to $(1\bar{1}0)$ plane.

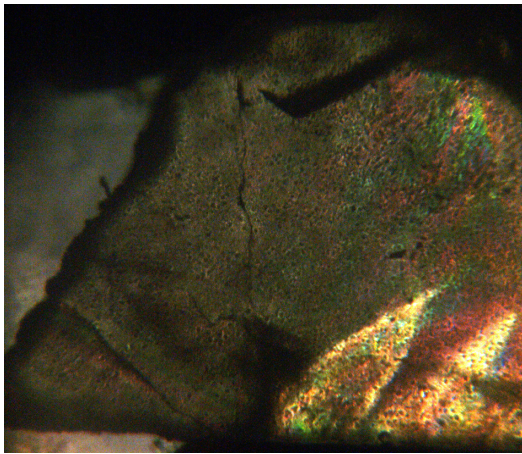


Fig. 4. Phase boundary in RTCS crystals ($x = 0.1$) of $\langle 111 \rangle$ orientation. The photograph corresponds to the temperature of PT into the FE phase.

Let us now remind that the deviations from mutually orthogonal orientation for the domain walls in the other FE langbeinites are of the same order of magnitude and they change their values, depending on specific crystal. Since we have not seen the appearance of FE domain structure, we conclude that no peculiarities typical for the domain structure in the mixed $K_2Cd_{2x}Mn_{2(1-x)}(SO_4)_3$ crystals is observed here, except for that the orientation of the phase boundary in the present case is similar to that of the domain walls in $K_2Cd_{2x}Mn_{2(1-x)}(SO_4)_3$ crystals. Following from the results presented above, one can conclude that two pairs of conjugated phase boundaries are observed in the langbeinites at the FE PT:

(1) a pair of conjugated walls with the $\{110\}$ orientation. Their orientation coincides

with that of the domain walls in the other FE langbeinites. It is explained in terms of the residual walls, which exist between enantiomorphous twins appearing due to hypothetical PT with the symmetry change $\bar{4}3mF23$;

(2) a pair of conjugated walls with the orientation that deviates from the $\{110\}$ plane by some angle. The latter probably depends on the orientation minimum of elastic energy of the phase boundary. These phase boundaries have the same orientation as the domain walls inclined to the $\{110\}$ planes.

Let us now analyze the elastic energy minimum depending on the orientation of phase boundary. Unfortunately, there are no literature data on the temperature dependence of lattice parameters for the RTCS crystals, though those data are available for $K_2Cd_2(SO_4)_3$ and $K_2Mn_2(SO_4)_3$ crystals [18,19]. Regarding the orientation angles of the phase boundaries (or the domain walls) in the crystals under interest, we refer a reader to our recent papers [9,13].

Computer simulations

Let us consider the phase boundary as an infinitely thin layer that separates the regions of cubic paraelastic phase of the 23 symmetry and single-domain state of the FE phase 222. The elastic energy density can be written in a usual way:

$$W = \frac{1}{2} C_{ijkl} \Delta e_{ij} \Delta e_{kl}, \quad (1)$$

where C_{ijkl} are the components of elastic stiffness tensor at T_c and Δe_{ij} denote the differences between the deformations that appear at the phase boundary due to elastic non-compatibility. Actually, the deformation differences at the phase boundary are equal to spontaneous deformations ($\Delta e_{ij} = e^s_{ij}$), because the deformations can be normalized to zero for the paraelastic phase. When solving problem of the most energy-wise preferable orientation of

the phase boundaries, one should utilize two-dimensional ‘projections’ of spontaneous deformation and elastic stiffness coefficient tensors. At the same time, the orientation of the plane that crosses indicative surfaces of these tensors is unknown in advance. Let us consider two Cartesian coordinate systems, one of which is coupled with crystallographic frame of reference and the other one is rotated by some angle. Z' axis of the rotated system is directed along the vector normal to the plane searched for. Now we rewrite the elastic stiffness and spontaneous deformation tensors in the rotated coordinate system $X'Y'Z'$ in terms of the transformation matrix a_{ij} :

$$C'_{ijkl} = a_{im} a_{jn} a_{ko} a_{lp} C_{mnop}, \quad (2)$$

$$e'_{ij} = a_{im} a_{jn} e_{mn}, \quad (3)$$

where the components a_{ij} are as follows:

$$\begin{aligned} a_{11} &= \cos \beta \cos \gamma \\ a_{12} &= -\cos \beta \sin \gamma \\ a_{13} &= \sin \beta \\ a_{21} &= \sin \alpha \sin \beta \cos \gamma + \cos \alpha \sin \gamma \\ a_{22} &= -\sin \alpha \sin \beta \sin \gamma + \cos \alpha \cos \gamma \\ a_{23} &= -\sin \alpha \cos \beta \\ a_{31} &= -\cos \alpha \sin \beta \cos \gamma + \sin \alpha \sin \gamma \\ a_{32} &= \cos \alpha \sin \beta \sin \gamma + \sin \alpha \cos \gamma \\ a_{33} &= \cos \alpha \cos \beta \end{aligned} \quad (4)$$

Here α , β and γ mean the angles of rotation of the new coordinate system respectively around X , Y and Z axes of the crystallographic system. After crossing indicating surfaces of

these tensors by the plane $Z'=0$, one can find the ‘projection’ tensors corresponding to the phase boundary plane. The components of the spontaneous deformation tensor may be easily calculated from the temperature dependences of the lattice parameters of $K_2\text{Cd}_2(\text{SO}_4)_3$ crystals, using the formulae

$$e_{11} = \frac{a-a_0}{a_0}, \quad e_{22} = \frac{b-a_0}{a_0}, \quad e_{33} = \frac{c-a_0}{a_0}, \quad (5)$$

where a_0 is the lattice parameter of the cubic phase in the vicinity of T_c and a, b, c the lattice parameters of the orthorhombic phase in the vicinity of T_c . Close to T_c , the lattice parameters, the spontaneous deformation and the elastic stiffness components [20] for $K_2\text{Cd}_2(\text{SO}_4)_3$ crystals are as follows: $a_0 = 10.27\text{\AA}$, $a = 10.26\text{\AA}$, $b = 10.29\text{\AA}$, $c = 10.26\text{\AA}$, $e_{11} = -0.97 \times 10^{-3}$, $e_{22} = 1.95 \times 10^{-3}$, $e_{33} = -4.87 \times 10^{-3}$ and $C_{11} = 5.45 \times 10^{10} \text{ m}^2 / \text{N}$, $C_{12} = 2.45 \times 10^{10} \text{ m}^2 / \text{N}$, $C_{44} = 1.85 \times 10^{10} \text{ m}^2 / \text{N}$. Inserting these components into Eq. (1) and using computer simulations, one can determine the phase boundary orientation angles that correspond to the condition of minimum of elastic non-compatibility energy. The separate components of the elastic stiffness tensor for $K_2\text{Mn}_2(\text{SO}_4)_3$ crystals are not available. Dependences of the elastic energy density on the angles of phase boundary plane orientation for $K_2\text{Cd}_2(\text{SO}_4)_3$ crystals are presented in Fig. 5.

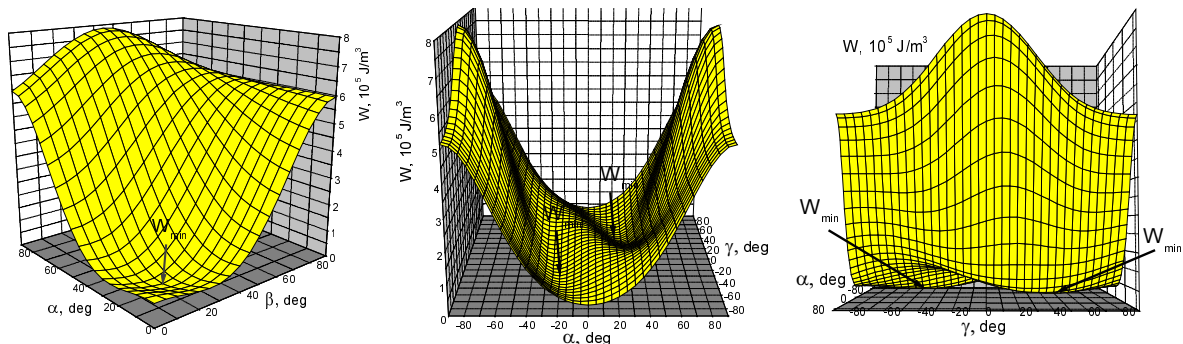


Fig. 5. Angular dependences of elastic energy density of the phase boundary for $K_2\text{Cd}_2(\text{SO}_4)_3$ crystals.

As seen from Fig. 5, the dependence of the elastic energy density caused by deformation non-compatibility acquires minimal values ($W_{\min} = 2.1 \times 10^4 \text{ J/m}^3$) at 17° for $K_2Cd_2(SO_4)_3$ crystals. The values obtained experimentally for the inclined domain walls are $12^\circ \pm 5^\circ$ for $K_2Cd_2(SO_4)_3$. One has to account for that the errors concerned with the lattice parameters and the elastic stiffness coefficients, which are used in our calculations, might be rather large exactly at T_c . Then one can conclude that we have obtained a fairly good agreement between the calculated and measured orientation angles for the phase boundaries.

Conclusions

Summing up the results of this study and involving the appropriate results of our recent works, we have to consider the two different scenarios of the FE PT in langbeinites:

1. At the direct PT with the symmetry change $23F222$, the domain structure most often appears in the form of heterophase structure, i.e. a sandwich-like structure consisting of layers of FE domains and paraelastic phase. The two types of conjugated domain walls can appear in this process:

(a) a pair of conjugated walls with the $\{110\}$ orientation. The orientation of these walls coincides with the orientation of domain walls in the other FE langbeinites. It is explained in terms of residual walls existing between enantiomorphous twins that appear due to hypothetical PT with the symmetry change $\bar{4}3mF23$;

(b) a type of domain walls that play simultaneously a part of phase boundaries. There is a pair of these conjugated walls, with the orientation deviating from the $\{110\}$ planes. The value of the deviation angle depends on the orientation minimum of elastic energy of the phase boundary. These phase boundaries have the same orientation as the domain walls inclined with respect to the $\{110\}$ planes.

2. At the indirect PT into FE phase ($23F2F1F222$), the crystal is usually transformed into single-domain state. The orientation of the phase boundary is determined by the minimum of elastic non-compatibility energy between the high-temperature phase and the FE phase.

Besides, we have also shown in the present paper that $Rb_{2x}Tl_{2(1-x)}Cd_2(SO_4)_3$ crystals usually become single-domain at the PT into FE phase. The phase boundary movement appears during this PT, which testifies a first-order character of the PT. Then the phase boundary has either the exact $\{110\}$ orientation or deviates from this orientation by the angle of $\sim 10^\circ$.

Acknowledgement

The authors acknowledge financial support of this study from the Ministry of Education and Science of Ukraine (Project N0106U000615).

References

1. Zambononi F. and Carobbi G. *Pend. Acad. Sci. Fis. Mat. Napoli* **20** (1923) 123.
2. Gattow G. and Zemann J.Z. *Anorg. Algem. Chem.* **293** (1958) 233.
3. Mc.Murdie H.F., Morris M.C., de Groot J. and Swanson H.E. *J. Res. Nat. Bureau Standarts.- A. Physics and Chem.* **75A** (1971) 435.
4. Dvorak V. *Phys. Stat. Sol. (b)* **52** (1972) 93.
5. Dvorak V. *Phys. Stat. Sol. (b)* **66** (1974) K87.
6. Say A., Sveleba S., Teslyuk I., Martynyuk-Lototska I., Girnyk I. and Vlokh R. *Ukr. J. Phys. Opt.* **7** (2006) 41.
7. Vlokh R., Girnyk I., Martynyuk-Lototska I., Czaplá Z., Dacko S. and Kosturek B. *Ferroelectrics* **303** (2004) 51.
8. Sapriel J. *Phys. Rev. B* **12** (1975) 5128.
9. Vlokh R., Skab I., Vlokh O. and Uesu Y. *Ukr. J. Phys. Opt.* **2** (2001) 148.
10. Vlokh R., Girnyk I., Vlokh O.V., Skab I., Say A. and Uesu Y. *Ukr. J. Phys. Opt.* **5** (2004) 141.

11. Vlokh R., Skab I., Vlokh O., Uesu Y. and Yamada Y. *Ferroelectrics* **242** (2000) 47.
12. Vlokh R., Vlokh O., Skab I. and Romanyuk M. *Ukr. J. Phys.* **43** (1998) 80 (in Ukrainian).
13. Vlokh R., Uesu Y., Yamada Y., Skab I. and Vlokh O.V. *J. Phys. Soc. Jap.* **67** (1998) 3335.
14. Vlokh R.O., Vlokh O.V., Kabelka H. and Warhanek H. *Ferroelectrics* **190** (1997) 89.
15. Vlokh R., Kabelka H., Warhanek H., Skab I. and Vlokh O.V. *Phys. Stat. Sol.(a)* **168** (1998) 397.
16. Dudnik E.F. and Shuvalov L.A. *Ferroelectrics* **98** (1989) 207.
17. R.Vlokh, I.Skab, I.Girnyk, Z.Czapla, S.Dacko and B.Kosturek *Ukr. J. Phys. Opt.* **1** (2000) 28.
18. Lissalde F., Abrahams S.C., Bernstein J.L. and Nassau K. *J. Appl. Phys.* **50** (1979) 845.
19. Itoh K., Ukeda T. and Nakamura E. *J. Phys. Soc. Jap.* **61** (1992) 4657.
20. Antonenko A.M., Volnyanski M.D. and Pozdeev V.G. *Fiz. Tverd. Tela* **25** (1983) 1849 (in Russian).